Gear test rig for health monitoring and quasi static- and dynamic testing; design, construction and first results

F. L. J. van der Linden
German Aerospace Center (DLR), Germany

ABSTRACT
This paper describesthe design and construction of a static and dynamic gear transmission test rig to analyse the position dependent elasticity, losses and transmission errors under varying circumstances. These data is important for system simulations and development of health monitoring algorithms predicting system behaviour with faults. A detailed description of the test rig is given. Example measurements of gear elasticity and losses are presented.

1 INTRODUCTION

Gear transmissions, although extensivelystudied, are still not fully understood. Especially the behaviour of transmissions with faults, manufacturing imperfections and also gear stiction are still under investigation. For the development of health monitoring algorithmsto monitor gear transmissions, it is important to know the exact behaviour of such a damaged gear. The results of the presented tests can be included in simulation models to predict the system behaviour and the effectiveness of health monitoring algorithms.
The work done until 1988 on gear modelling is very well described in the review paper of Özgüven and Houser (1). In more recent work, much attention is paid to varying tooth stiffness. Extensive research on the field of the effect of stiffness is done by Kahraman and Singh (2, 3), Kar and Mohanty(4, 5), Parey and Tandon(6–8),Guo and Parker (9), as well as Fernandez del Rincon et al. (10). They all acknowledge that varying tooth stiffness is very important in gear studies. One of the most recent efforts in experimentally measuring the tooth stiffness is by Hotait and Kahraman(11). Velex and Martar(12) have shown the importance of transmission errors. The role of varying tooth friction on gear excitement is shown by Velex and Cahouet(13).
There are many factors which influence gear transmissions: load, position, speed, temperature and even vibrations can influence the (local) properties. To effectively measure all these influences, a test rig has been developed. The results of the tests will be used to aid model development and validation.
In this paper, the setup of a small transmission test rig with ratio 1:3 using grounded straight tooth of quality 7e25 is presented. The goal of the test rig is to analyse the elasticity of the tooth contact under varying circumstances and fault scenarios. The rig is designed to be multi-functional; also gear position dependant losses (14)canbe measured. Testing of health monitoring algorithms is also one of the goals of the rig.

2 TESTRIG DESCRIPTION

In this chapter the test rig setup is discussed. The presented test rig is shown inthe schematic overview in Figure 1 and as designed and constructed in Figure 2. The rig is usestwo permanent magnet synchronous motors which are controlled by inverters. This configuration enables to prescribethe position and the load of the gearbox simultaneously. Each motor is connected to a moment sensor and finally to the gear box using torsional stiff couplings.To monitor the gear connection, an acceleration sensor as well as an acoustic emission (AE) sensor is used. Furthermore the housing, environment and oil temperature are measured.

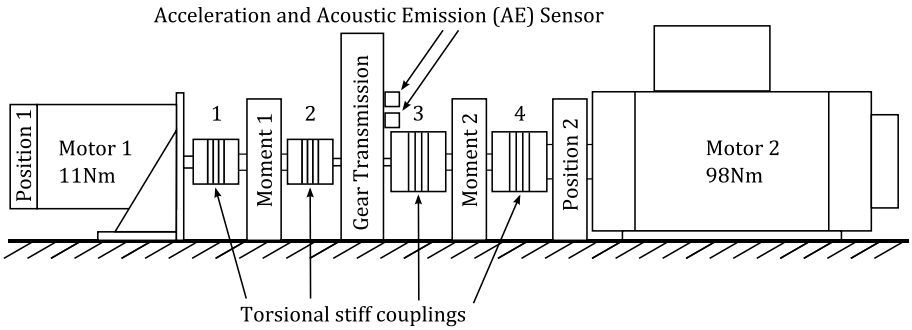

Figure 1. Schematic overview of test rig

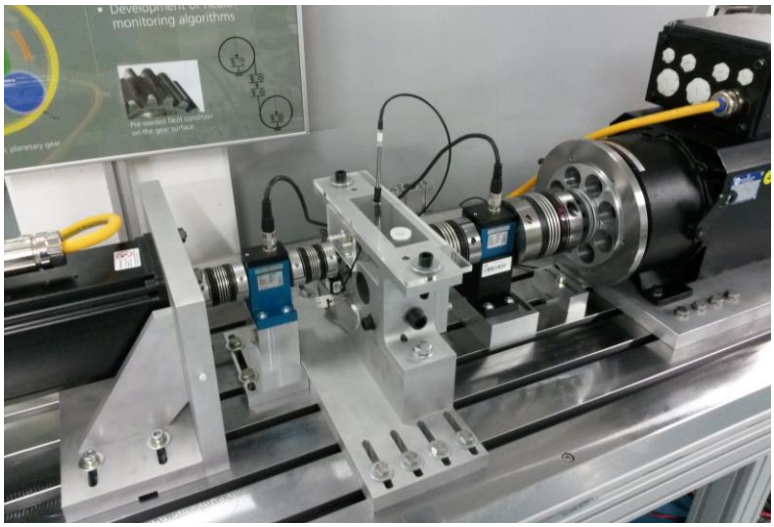

Figure 2. Test rig as currently operated at DLR

2.1 Test Rig setup

The test rig is based on an aluminium frame supporting the base of the rig; a6cm thick steel plate with DIN 650 size 16 T-slots to eliminate any twisting of the support. To connect all parts to this plate, adapters are constructed to fix the components to the T-slots. The adaptersare aligned to the nuts using tenons (DIN 6322 / DIN 6323).In this

way it possible to align the parts on the plate with high accuracy and very high flexibility.
Before the T-slots and tenons were added to the test rig, it has been proven very difficult to achieve a good alignment of the parts. Furthermore the assembly and disassembly was more complicated. The base plate has shown to be of great influence on the measurements, as the twist of individually connected aluminium profiles proved to lead to measurement errors.

2.2 Sensor setup

The rig can be used for many applications like elasticity measurements, friction measurement and health monitoring algorithm testing. These different applications call for different sensors. In Table 1an overview of all sensors and their accuracy is shown.

Sensor description	Accuracy	Bandwidth	Range	Brand/ Type number
Positionssensor 1	± 7'' differential nonlinearity, ± 45'' system	>12000 RPM	-	Stegman / SinCos SRS 50
Positionssensor 2	± 5'' differential nonlinearity, ± 12'' system	> 3000 RPM	-	Heidenhain / ERM220
Moment sensor 1	<±0,2 % nonliniarity	3 kHz @3dB	20Nm	Kistler / 4502A20RAU
Moment sensor 2	<±0,2 % nonliniarity	3 kHz @3dB	100Nm	Kistler / 4502A100RA
Acceleration sensor	<2% sensitivity	0.3-10000Hz	±10g	Crossbow / CLX10HF3
Acoustic Emission (AE) sensor		100-900kHz	~75 dB re 1V/µbar	Vallen/ ASCO-PH5 & VS900-M
Temperature sensor (oil)	<0.1% nonlinearity	-	0-150˚C	PT100
Temperature sensor (housing)	<0.1% nonlinearity	-	0-150˚C	PT100
Temperature sensor (environment)	<0.1% nonlinearity	-	0-150˚C	PT100

Table 1. Sensors of the test rig

The sensors are selected based on their accuracy and bandwidth. The high bandwidth of the sensors enables the measurement of high frequency effects like tooth meshing effects.

2.3 Moment sensor stiffness properties

The moment sensors used in the test rig are based on strain gauge technology. Therefore the sensors have a non-negligible stiffness.

Sensor	Torsional Stiffness	Measurement range
1	4.58kNm/rad	20Nm
2	28.6kNm/rad	100Nm

Table 2.Stiffness properties of the moment sensors

2.4 Motor properties

The electric motors used in the test rig are permanent magnet synchronous motors controlled by inverters. Both motors can be operated in current, speed or position control mode. Furthermore it is possible to directly control an input using an internal PID controller. This makes it possible to have a torque control mode too by using feedback from the moment sensors.The motor properties are listed in Table 3.

Motor description	Nominal power	Nominal torque	Nominal current	Max speed	Inertia	Brand/ type number
Motor 1	5.2 kW	11.0 Nm	10.0 A	4500 RPM	1.65e-3 kgm^2	Baumueller / DSD071L64U45-5
Motor 2	12.4 kW	98 Nm	22.5 A	1200 RPM	58e-3 kgm^2	Baumueller / DS132M54U12-5

Table 3. Properties of the motors

Motor 2 is selectedsuch to enable test gears up to a gear ratio of 1:8. For gears with a gear ratio smaller thanapproximately 1:3, motor 2 limits the maximal speed to 1200 RPM.

2.5 Inverter properties

The inverters to control the motors use field control with position feedback. Since in the presented configuration always one motor is used in generator mode, the generated power is returned to the drive motor over the DC link. Using this setup, the power consumption of the test rig is limited, even under high load conditions.

Inverter description	Nominal power	Switching frequency	Brand/ type number
Inverter 1	11A	4kHz	Baumueller / BM4423-STO-01200-03
Inverter 2	30 A	4kHz	Baumueller / BM4433-SIO-01200-03

Table 4. Properties of the inverters

2.6 Coupling properties

Bellow couplings are used in the test rig because they are rotational symmetric and therefore the stiffness and torque loss areindependent from the motor position.

Coupling	Torsional stiffness	Inertia	Brand/ Type number
1, 2	39e3Nm/rad	0.14e-3kgm^2	R+W / BKH / 30 /69
3	175e3Nm/rad	1.9e-3 kgm^2	R+W / BK2 / 150 /95
4	450e3Nm/rad	7.6e-3 kgm^2	R+W / BK2 / 300 /111

Table 5. Properties of the couplings

2.7 Transmission properties

The gear wheels used in the test rig are standard, straight cut gears of module 1. A transmission ratio $i = 3$is selected to make sure that always the same teeth are meshing. Although whole number transmissions ratios are usually avoided to assure even meshing conditions, this simplifies the analysis. To avoid play of the gears on the axle, a press fit is used to connect the gears to the axle.

Gear	Number ofteeth	Face width	Module	Tooth quality	Material	Surface treatment
A	20	10mm	1.0	7e25	Steel (16MnCr5)	Case-hardened, grinded, HRC 58±2
B	60	10mm	1.0	7e25	Steel (16MnCr5)	Case-hardened, grinded, HRC 58±2

Table 6. Properties of the gears

Both gear axles are supported by ball bearings. The gears and bearings are lubricated with Meguin CLP320 gear oil for the low speed elasticity measurements. This is a thick gear oil to assure a good lubrication at low speeds.

2.8 Drive shaft properties

The shaftsof both gear wheels are made from steel. Their properties can be found in Table 7. The multiple length and dimensions found in this table are caused by a stepped shaft. For the stiffness calculation, the length up to the gear wheel is measured, as only this part is torsional loaded. For the calculations, a shear modulus of 79.3GPa is selected for normal steels.

Axle	Material	Length between coupling and gear	Diameter	Stiffness
A	Steel	32mm 12mm	10mm 12mm	16 kN/rad
B	Steel	24mm 12mm 19mm	18mm 15mm 14mm	65kN/rad

Table 7. Properties of the axis

2.9 Train stiffness

To calculate the stiffness of the gear contact, the stiffness of the complete gear train without the gear contact must be known. This train stiffness is obtained by lumping the stiffness of all parts to the side of motor 1 using the gear ratio i is given:

$$\frac{1}{c_{lump}} = \frac{1}{c_{coupl\,1}} + \frac{1}{c_{coupl\,2}} + \frac{1}{i^2 c_{coupl\,3}} + \frac{1}{i^2 c_{coupl\,4}} + \frac{1}{c_{sens\,1}} + \frac{1}{i^2 c_{sens\,2}} + \frac{1}{c_{axle\,1}} + \frac{1}{i^2 c_{axle\,2}} \qquad (1)$$

Using the properties from Table 2, Table 5 and Table 7 the total lumped gear train stiffness at the side of motor 1 is 3.0 kN/rad.

2.10 Signal acquisition and data logging

The test rig is controlled and the measurement data is logged using a real-time Target/Hostsystem using Labview. A standard PC (Xeon W3530, Quadcore, 2.8Hhz) with 3GB RAMis used as target PC. Two multifunction measurement cards measure the signals: a NI PCIe-6343 for the position sensors and signals used for control feedback,

and one NI-PC-6031E card for all signals without feedback (temperature, acceleration, Acoustic Emission (AE)).
All sensors(except the position sensors), are analogue sensors which are connected to the Target-PC using standard breakout boxes(NI BNC-2090 & NI BNC-2090A). All analogue sensor signals are low pass filtered at 1.8kHz with a first order analogue filter to avoid aliasing effects. These filters have been realized inside the breakout boxes before sampling of the signal using an RC filter with 2.69KΩ resistors and 33nF capacitors.The position sensor signals (quadrature encoder signals) are connected to the digital interfaces and decoded by the measurement cards.
All data are recorded in the streaming data logging format TDMS at 8kHz.

3 GEARSTIFFNESS AND LOSS MEASUREMENTS

To measure position- and load dependent stiffness, as well as the position and load dependent friction, the test rig controllers and measurements need to be reconfigured. It is chosen to command a constant velocity on motor 1, while controlling the load of motor 2 using feedback from the moment sensor 2 (see figure Figure 1). To obtain a load dependant elasticity, the load is increased stepwise on motor 2 every 3 revolutions. In Figure 3, an overview of a load scenario is depicted with a moment increase of 5 Nm in each step. For a higher resolution with respect to load, the load steps can be chosen smaller. For a typical measurement 0.1-0.3 Nm steps are used. Increasing the resolution of the moment steps will increase the measurement and calculation time.

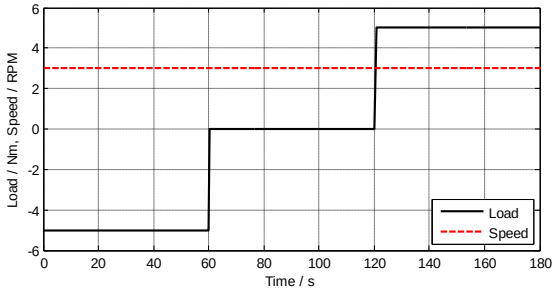

Figure 3. Commanded speed and load of the gear during a stiffness measurement

To avoid dynamic effects from the measurements, a small rotation velocity is selected.This eliminates high accelerations and enables to treat the measurements as quasi static measurements.

4 FIRST RESULTS

Position and load dependent stiffness and losses are important parameters for simulation models to predict gear performance and for the testing of health monitoring algorithms. In this Section is described how these measurements are carried out.
Using the setup discussed in Section 2combined with the measurement method described in Section 3, tests were run for a transmission with an artificially introduced fault. To this end, a tooth was removed from the gearwheel 1 (see Figure 4).
In the discussed measurement, the average speed of motor 1 was 3.1RPM and the stepsize of the moment was 0.3Nm. All measurement data is collected over 3 revolutions of motor 2.

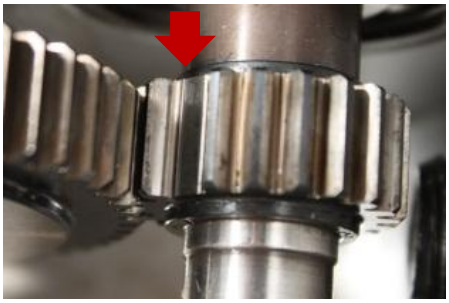

Figure 4. Artificially removed tooth

4.1 Gear stiffness

To calculate the stiffness of the gear transmission reduced to the side of motor 1, the relative motion of the gears must be known. This can be calculated as ($i = 3$):

$$\phi_{rel} = \phi_{motor\ 1} - i\phi_{motor\ 2} \tag{2}$$

This relative angle is resampled on an equidistant grid with 5000 grid points in the rotational direction and 400 grid points in the load direction using the function gridfit(15).InFigure 5, the relative angle of the gear transmission is shown as a function of speed and load. The broken tooth can be identified at 1/3, 2/3and 1 times the rotation of motor 2.

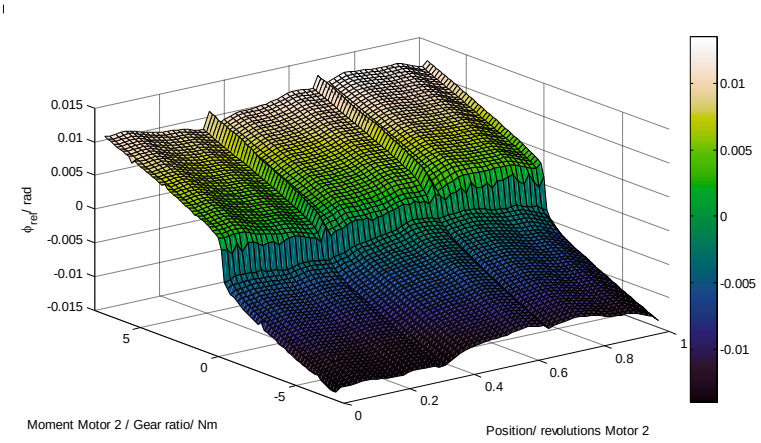

Figure 5. Equidistant grid of ϕ_{rel}, the relative angle of the sensors 1 and 2.

The stiffness of the gear transmission trainis given by taking the local derivative of this surface with respect to the load. Before calculating thederivative the data was smoothed using a 2 dimensional averaging filter over 0.06rad and 0.3Nm to suppress noise.
The results of these calculations can be seen inFigure 6.The stiffness increases with load. The stiffness at loads over 5 Nm is approximately 950N/rad. A lower stiffness is observed at the missing tooth as well as play at 0 Nm.

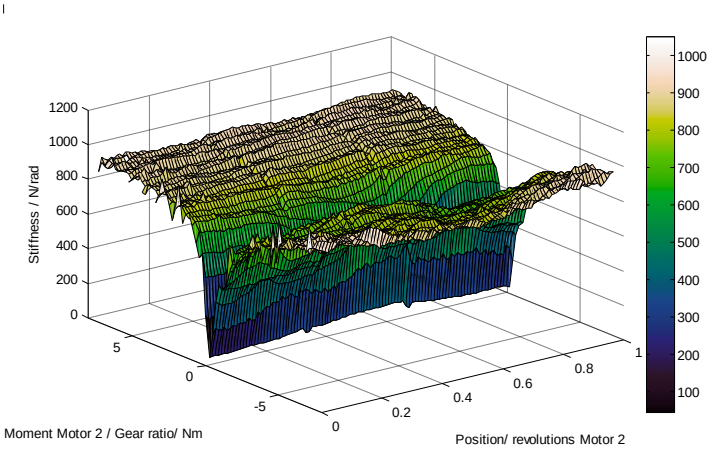

Figure 6. Gear Stiffness

4.2 Gear losses

Using the measurements from Section 4.1, the gear losses can be obtained by:

$$\tau_{loss} = \tau_{sensor,1} - \frac{\tau_{sensor,2}}{i} \tag{3}$$

The results of the measurements corrected for 0.138Nm mean drag losses at zero velocity are shown inFigure 7. The mean drag at zero load is assumed to be due to friction of the seals and splash losses and bearing drag load. Assuming this friction momentto be constant with varying load, the average loss at full load of 8Nm of motor 1 is 0.1Nm. This corresponds to an average loss of 1.25% in the gear tooth. These high gear losses are probably due to the low rotational speed of the motor.

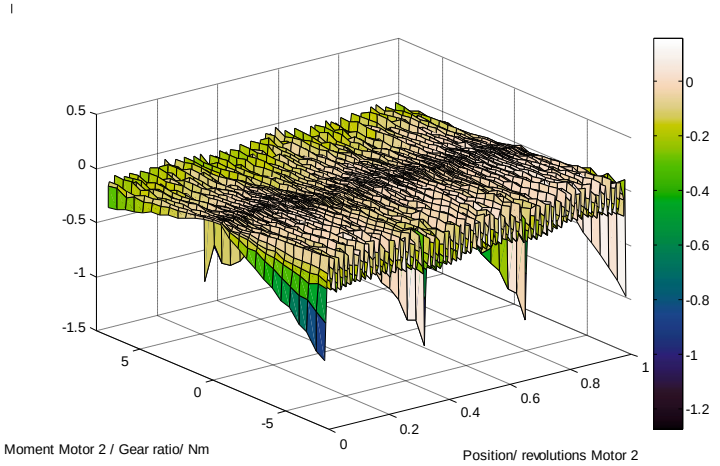

Figure 7.Corrected gear losses

5 CONCLUSION AND DISCUSSION

Atest rig to measure the position dependent elasticity, losses and position error is presented. All properties of the test rig with its components are thoroughly documented. The first results of the test rig are promising to be useful for system simulation models. The average stiffness and losses show a good correlation with results from literature.Tests of damaged components also deliverresults, which can be included in system simulations for the development of health monitoring algorithms.
The test rig is currently used to accurately measure stiffness and losses of gearboxes under varying circumstances. These measurements include damaged components and different lubrications. The presentedmeasurements are done using quasi-static measurements. In the future, also tests at normal operational speeds are planned.
During the development of the test rig, the accuracy of the position sensors proved to be crucial for the measurements as the stiffness variations are small. Approximations of the motor moments using the current proved to be unusable due to the varying motor constant with load and position and have been replaced with moment sensors. Furthermore a rigid base plate was found to be needed to avoid the influence of test rig twisting on the gear measurements.

6 BIBLIOGRAPHY

(1) H. NevzatÖzgüven and D. R. Houser, "Mathematical models used in gear dynamics - A review," *Journal of Sound and Vibration*, vol. 121, no. 3, pp. 383–411, Mar. 1988.

(2) A. Kahraman and R. Singh, "Non-linear dynamics of a spur gear pair," *Journal of Sound and Vibration*, vol. 142, no. 1, pp. 49–75, 1990.

(3) A. Kahraman and R. Singh, "Interactions between time-varying mesh stiffness and clearance non-linearities in a geared system," *Journal of Sound and Vibration*, vol. 146, no. 1, pp. 135–156, 1991.

(4) C. Kar and A. R. Mohanty, "Determination of time-varying contact length, friction force, torque and forces at the bearings in a helical gear system," *Journal of Sound and Vibration*, vol. 309, no. 1–2, pp. 307–319, Jan. 2008.

(5) C. Kar and A. R. Mohanty, "Vibration and current transient monitoring for gearbox fault detection using multiresolution Fourier transform," *Journal of Sound and Vibration*, vol. 311, no. 1–2, pp. 109–132, Mar. 2008.

(6) A. Parey, M. El Badaoui, F. Guillet, and N. Tandon, "Dynamic modelling of spur gear pair and application of empirical mode decomposition-based statistical analysis for early detection of localized tooth defect," *Journal of Sound and Vibration*, vol. 294, no. 3, pp. 547–561, Jun. 2006.

(7) A. Parey and N. Tandon, "Spur Gear Dynamic Models Including Defects: A Review," *The Shock and Vibration Digest*, vol. 35, pp. 465–478, 2003.

(8) A. Parey and N. Tandon, “Impact velocity modelling and signal processing of spur gear vibration for the estimation of defect size,” *Mechanical Systems and Signal Processing*, vol. 21, no. 1, pp. 234–243, Jan. 2007.

(9) Y. Guo and R. G. Parker, “Dynamic Analysis of Planetary Gears With Bearing Clearance,” *Journal of Computational and Nonlinear Dynamics*, vol. 7, no. 4, p. 41002, 2012.

(10) A. Fernandez del Rincon, F. Viadero, M. Iglesias, P. García, A. de-Juan, and R. Sancibrian, “A model for the study of meshing stiffness in spur gear transmissions,” *Mechanism and Machine Theory*, vol. 61, pp. 30–58, 2013.

(11) M. A. Hotait and A. Kahraman, “Experiments on the relationship between the dynamic transmission error and the dynamic stress factor of spur gear pairs,” *Mechanism and Machine Theory*, vol. 70, pp. 116–128, 2013.

(12) P. Velex and M. Maatar, “A mathematical model for analyzing the influence of shape deviations and mounting errors on gear dynamic behaviour,” *Journal of Sound and Vibration*, vol. 191, no. 5, pp. 629–660, Apr. 1996.

(13) P. Velex and V. Cahouet, “Experimental and Numerical Investigations on the Influence of Tooth Friction in Spur and Helical Gear Dynamics,” *Journal of Mechanical Design*, vol. 122, no. 4, p. 515, 2000.

(14) L. Márton and F. van der Linden, “Temperature dependent friction estimation: Application to lubricant health monitoring,” *Mechatronics*, vol. 22, no. 8, pp. 1078–1084, Dec. 2012.

(15) J. D’Errico, “Surface Fitting using gridfit,” *Matlab Central*, 2005. [Online]. Available: http://www.mathworks.de/matlabcentral/fileexchange/8998-surface-fitting-using-gridfit. [Accessed: 22-Apr-2014].